Cite this as: Inorganica Chimica Acta 434 (2015) 215–220

Synthesis and characterization of new mixed–valent Mn(II)/Mn(III) and mixed metal Ni/Mn complexes

M. Ledezma-Gairaud,[b] L. W. Pineda,[b] G. Aromí[a] and E. C. Sañudo[a*],

Microwave assisted synthesis and bench-top reactions are compared for Mn and Mn/Ni reaction systems with substituted salicylic acid (2-hydroxy-6-isopropyl-3-methylbenzoic-acid ($SALOH_2$). When Mn salts are used, the microwave assisted synthesis and the bench-top reaction afford the same product: the new octanuclear Mn(II)/Mn(III) complex $[Mn_8O_2(OMe)_2Cl_2(SALO)_6(MeOH)_4(H_2O)_2]$ (**1**). However, in a mixed metal Mn/Ni reaction the bench-top reaction results in the new heterometallic distorted cubane complexes $[Pr_2NH_2][Mn_2Ni_2(OH)_2(L_1)_2(SALO)_2(SALOH)_3]$; where L_1H = 3-dimethylamino-1-propanol, (**2**) and $[Pr_2NH_2][Mn_2Ni_2(OH)(OMe)_2(L_1)(MeCN)(SALO)_2(SALOH)_3]$ (**3**). The crystal structure and magnetic properties of the prepared complexes are presented.

1. Introduction

Transition metal coordination complexes possess interesting magnetic properties like for example single-molecule magnet (SMM) behavior, as first reported for $[Mn_{12}O_{12}(O_2CMe)_{16}(H_2O)_4]$ [1]. This dodecanuclear mixed-valent Mn complex was the first found to function as a magnet at the molecular level. Nanomagnets and SMMs are postulated as a molecular approach to nanomagnetism [2]. The interesting magnetic properties of high nuclearity coordination complexes and the possible future applications in information storage and processing technologies [3] have fueled researcher's interest toward the finding of alternate synthetic methods to new functional coordination complexes. The majority of polynuclear complexes of transition metals have been isolated at bench-top ambient conditions, [4] but since the early 2000's an increasing number of complexes have been synthesized by using heat and pressure by solvothermal [5] or microwave assisted reactions. Microwave assisted synthesis is a clean, cheap and convenient method of heating that can result in higher yields, shorter reaction times, and sometimes in the formation of completely new products. The use of sealed-vessel microwave reactors enables reaction mixtures to be heated rapidly to temperatures well above the boiling point of the solvent under atmospheric conditions. Such temperature profiles can sometimes be difficult, if not impossible to reproduce, using conventional conductive heating [6]. Microwave assisted synthesis has been widely used in the preparation of organic compounds[7] and has recently been extended to coordination chemistry and metal-organic frameworks (MOFs) [8-11]. In the field of coordination chemistry, Brechin *et al.* have reported several metal carboxylate clusters prepared under microwave-assisted reaction conditions, including Co_3, Ni_3, Mn_6 and Fe_8 [12]. These results highlight the advantages of this technique: fast reaction rates and short reaction times; high yields and high phase purity. In our group, we have had a important interest in microwave assisted synthesis and we have reported the isolation of Ni_8 and Ni_9 [13], Co_3, Ni_6 and Mn_4 complexes [14], which could not be prepared by traditional bench-top synthesis. Furthermore, a comparative study of a mixed metal Mn/Ni system using 3,5-di*tert*butylsalicylic acid in bench-top and microwave assisted conditions [15] showed that the product from the bench-top reaction (Mn_5Ni_4) is clearly different from the product using microwave radiation, (Mn_7). Salicylic acid displays two good coordination sites, the phenol group and the carboxylato group. In this paper we combine our interest in microwave assisted synthesis applied to coordination complexes and our previous results with substituted salicylic acids, to study a Mn and Mn/Ni system under bench-top and microwave conditions using the substituted salicylic acid 2-hydroxy-6-isopropyl-3-methylbenzoic-acid ($SALOH_2$). In particular we have chosen the aliphatic substituents due to the low solubility of salicylic acid and its complexes, which prevents proper characterization and purification of the prepared species. The alkyl groups provide excellent solubility, favor crystallization and could be used to graft the prepared complexes on surfaces.

1. Experimental

2.1 Materials and methods

All chemicals and solvents were purchased from commercial sources and used as received. Microwave assisted reactions were done in a Discover System (CEM Corp.) microwave reactor. In the text and experimental section 2-hydroxy-6-isopropyl-3-methylbenzoic acid is $SALOH_2$, its mono-deprotonated form is SALOH (with a -1 negative charge) and its bi-deprotonated form is SALO (with a -2 negative charge); L_1H = 3-dimethylamino-1-propanol, its deprotonated form is L_1.

Elemental analyses were performed at the Serveis Científico-tècnics of the Universitat de Barcelona (CCiTUB). Magnetic measurements were performed at the Magnetic Measurements Unit of the CCiTUB, on a Quantum Design MPMS XL SQUID magnetometer equipped with a 5 T magnet. The data were corrected for TIP and the diamagnetic corrections were calculated using Pascal's constants. Infra Red spectra were collected on an AVATAR 330 FT-IR from Thermo scientific and on a Perkin Elmer, Spectrum 1000 FT. Single

crystal diffraction data for **1**·2C_2H_3N·5CH_4O·2H_2O; **2**·3CH_3CN·CH_3OH and **3**·CH_3CN·H_2O**,** were collected on a Bruker APEXII SMART diffractometer using a microfocus Molybdenum kα radiation source. The structures were solved by direct methods (SHELXS97) and refined on F^2 (SHELX-97). Hydrogen atoms were included on calculated positions, riding on their carrier atoms. Induced coupled plasma (ICP) measurements were performed at Centro de Investigación en Electroquímica y Energía Química, CELEQ; Universidad de Costa Rica on a Perkin Elmer Plasma 400 Emission Spectrometer with optical detector. The samples were first digested in nitric acid to dissolve them and the results were obtained from comparison with a calibration curve.

2.2 Synthesis

2.2.1 [$Mn_8O_2(MeO)_2Cl_2(SALO)_6(MeOH)_4(H_2O)_2$] **(1):** A solution of $MnCl_2$·4 H_2O (0.10 g; 0.51 mmol) in MeCN/MeOH (4:1 mL) was treated with 2-hydroxy-6-isopropyl-3-methylbenzoic acid, $SALOH_2$ (0.082 g, 0.42 mmol), 3-dimethylamino-1-propanol (58 µL, 0.49 mmol) and $HNPr_2$ (58 µL, 0.42 mmol). The reaction mixture was placed into the reactor cavity applying a 250 W microwave pulse for 5 min at 140 ºC. A small amount of precipitate was filtered off after cooling. The solution was allowed to stand for two weeks at room temperature resulting in single crystals of complex **1**. Yield: 0.030 g (23%). Elemental analyses calculated for **1**•8H_2O•1/2C_2H_3N: C, 42.02; H, 5.58; N, 0.33 %. Found: C, 41.36; H, 4.82; N, 0.35 %. Selected IR data (KBr, cm^{-1}): 3430 (br, s); 2966 (s), 2870 (w); 1593 (s); 1571 (s); 1465 (m); 1400 (s); 1246 (m); 1063 (w); 1020 (m); 971 (m); 871 (w); 819 (m); 790 (w); 752 (w); 654 (m); 566 (m).

2.2.2 [Pr_2NH_2][$Mn_2Ni_2(OH)_2(L_1)_2(SALO)_2(SALOH)_3$] (2): A solution of $MnCl_2$•4 H_2O (0.050 g, 0.25 mmol); $NiCl_2$•6 H_2O (0.050 g, 0.21 mmol), in MeCN (8 mL) and MeOH (2 mL) was treated with 2–hydroxy–6–isopropyl–3–methylbenzoic acid (0.082 g, 0.42 mmol), 3–dimethylamino–1–propanol (58 µL, 0.49 mmol) and $HNPr_2$ (58 µL, 0.42 mmol). The musk green solution was stirred for 1 h, and allowed to stand at room temperature affording block green single crystals by slow solvent evaporation. Yield: 0.010 g (5%). Anal. Calcd. (%) for **4**•2CH_3CN: C, 54.32; H, 6.12; N, 3.17. Found: C, 54.95; H, 6.90; N, 3.23. Selected IR data (KBr, cm^{-1}): 3422 (br, m); 2965 (s); 2869 (m); 1571 (s); 1459 (s); 1398 (s); 1384 (s); 1330 (s); 1243 (s); 1185 (m); 1168 (m); 1044 (m); 1017(s); 970 (m); 945 (m); 822 (m); 809 (m); 776 (m); 676 (m); 647 (m); 652 (m); 607 (m); 521(m).

2.2.3 [Pr_2NH_2][$Mn_2Ni_2(OH)(OMe)_2(L_1)(MeCN)(SALO)_2(SALOH)_3$] (3): A solution of $MnCl_2$•4 H_2O (0.0515 g, 0.261 mmol); and $NiCl_2$•6 H_2O (0.0515 g, 0.217 mmol), in MeCN (8 mL) and MeOH (2 mL) was treated with 2–hydroxy–6–isopropyl–3 –methylbenzoic acid (0.0820 g, 0.422 mmol), 3–dimethylamino–1–propanol (58 µL, 0.49 mmol) and $HNPr_2$ (58 µL, 0.42 mmol). The musk green solution was initially stirred 1 h, and allowed to stand at ambient temperature for three months affording plate green single crystals by slow solvent evaporation. Yield: 0.040 g (20%). Anal. Calcd. (%) for **4**•CH_3CN•H_2O**:** C, 55.12; H, 6.49; N, 3.57. Found: C, 55.00; H, 6.90; N, 3.29. Selected IR data (KBr, cm^{-1}): 3406 (br, s); 2964 (s); 1573 (s); 1461 (s); 1398 (s); 1332 (s); 1245 (s); 1018 (s); 965 (m); 823 (m); 783 (m); 541 (m).

2. Results and Discussion

3.1 Synthesis

Substituted salicylic acid derivatives have been used in order to obtain soluble new mixed-valent and mixed-metal high-nuclearity coordination complexes. The use of salicylic acid is well known in coordination chemistry and has afforded several complexes like for example [$Mn_9O_4(O_2CPh)_8(sal)_4(salH_2)(py)_4$] [16]. The salicylato ligand has several possible coordination modes to one or more metal centers, making it a great candidate for the synthesis of high-nuclearity complexes, some of these coordination modes are shown in Scheme 1. Thus, we have chosen the commercially available substituted salicylic acid 2-hydroxy-6-isopropyl-3-methylbenzoic acid ($SALOH_2$ from now on). In our group we had previously worked with 2-hydroxy-6-isopropyl-3-methylbenzoic acid, obtaining promising results in Ni(II) chemistry. As a co-ligand we have used 3-dimethylamino-1-propanol, a very flexible ligand that can help in the formation of high-nuclearity species which we have extensively used in our group. The microwave heating of manganese chloride with $SALOH_2$ and 3-dimethylamino-1-propanol in presence of $HNPr_2$ in a solvent mixture of MeCN/ MeOH affords a dark brown solution that subsequently leads to complex **1** in moderate yield of pure large crystals. The product obtained is [$Mn_8O_2(OMe)_2Cl_2(SALO)_6(MeOH)_4(H_2O)_2$] (**1**), an octanuclear mixed-valent Mn(II)/Mn(III) complex with chloride bridges and completely deprotonated SALO ligands. The aminoalcohol used in the reaction is not present in the final product, as we have previously observed in similar reactions [17]. The role of this organic compound along with the weak base in the reaction is probably to avoid precipitation of large amounts of manganese oxides. The weak base $HNPr_2$ can be replaced by NEt_3 to obtain complex **1** in similar yield, but reactions without the aminoalcohol resulted in large amounts of insoluble manganese oxides and intractable mixtures. Usually, the microwave-assisted reaction affords products that cannot be obtained in bench-top conditions; however this is not the case for this reaction system. A precipitate obtained from the same reaction to obtain complex **1** in regular bench-top conditions showed IR spectra similar to complex **1** contaminated by large amounts of manganese oxides. This was also reflected in elemental analyses of the precipitates that displayed very low amounts of C (< 20%). Even though the aliphatic substituents of $SALOH_2$ greatly increase the solubility of its coordination complexes, the octanuclear complex **1** has limited solubility and separation from the oxides and other by-products was not straightforward. Recrystallization attempts of the precipitates were unsuccessful. In this case, the microwave assisted synthesis results in the isolation of pure crystalline complex **1** that could not be obtained by other more conventional methods. The magnetic properties of the complex **1** revealed antiferromagnetic coupling (vide infra), and given our interest in magnetism and magnetic materials, we decided to try to tune them. Two strategies could be followed to tune the magnetic properties of this complex: one would be to replace the Mn(II) sites by Ni(II), thus increasing the anisotropy of the system, the other clear strategy would be to replace the chloro bridges by end-on azido bridges, which are known to favor ferromagnetic coupling [18], but the products were not the expected ones.

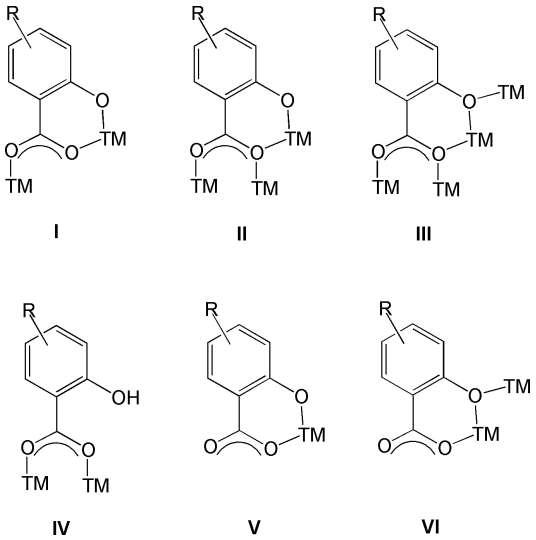

Scheme 1

The reaction of the mixed-metal Mn/Ni system was studied in normal bench-top conditions. In this case, the product obtained was not an octanuclear compound as expected from the analogous Mn-only reaction system, but the mixed-metal Mn_2Ni_2 tetranuclear complexes **2** and **3** which also contain two or one aminoalcohol ligands coordinated to the metals. Complexes **2** and **3** have a protonated dipropylamine counterion necessary for crystallization and charge balance. Only in one case complex **3**, with only one aminoalcohol ligand, was obtained. Complex **3** contains one coordinated MeCN and one bridging aminoalcohol ligand, but its preparation could not be reproduced. This again shows the complexity of reaction systems leading to high nuclearity coordination complexes: small changes, like for example oscillations in room temperature or solvent hydration levels, can be the cause for the isolation of complex **3** and not the usual product from the reaction, complex **2**.

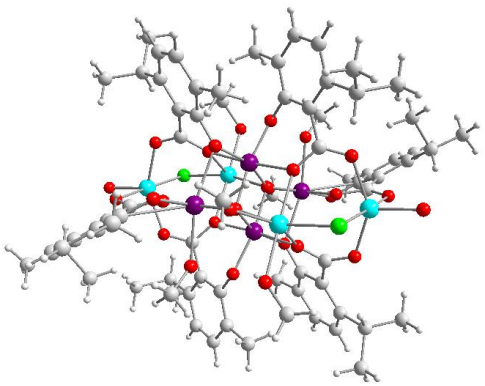

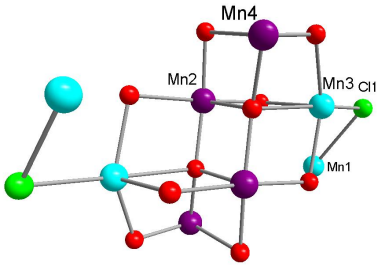

Figure 1. (top) Crystal structure of complex **1**. (bottom) The Mn–O core of complex **1**. Carbon: grey, hydrogen: light grey, oxygen: red, chloride: green, Mn(II): cyan, Mn(III): purple (color online).

Thus, for a Mn only system, microwave assisted synthesis facilitates the isolation of one pure product in crystalline form, while classic bench-top reactions favor the formation of by-products and manganese oxides which greatly hinder the purification of the product. However, when a mixed metal system of Mn/Ni is used, the species obtained by microwave-assisted synthesis are entirely different from the species obtained in classic bench-top reactions. Once again, the microwave assisted synthesis is an outstanding choice for the preparation of high-nuclearity coordination complexes, that has as main advantages short reaction times, small amounts of solvents (< 5 mL, thus reduction of organic solvent residues contaminated with heavy metals) and the isolation of pure, crystalline products.

3.2 Description of crystal structures

Data collection and structural parameters for **1, 2,** and **3** can be found in Table 1. The crystal structure of the complex $[Mn_8O_2(OMe)_2Cl_2(SALO)_6(MeO)_4(H_2O)_2]$ (**1**) is shown in Figure 1. Complex **1** crystallizes in the Triclinic space group P-1. The asymmetric unit consists of half a molecule, which is sitting on a crystallographic inversion center and several disordered solvents molecules (water, acetonitrile and methanol). The structure of complex **1** consists of a $[Mn_8(\mu_2\text{-}O)_8(\mu_4\text{-}O)_2(\mu_2\text{-}Cl)_2]$ core featuring four Mn(III) and four Mn(II) ions. Mn1 and Mn3 are in the oxidation state Mn(II) and Mn2 and Mn4 are in the oxidation state Mn(III).

The central part of the ladder, formed by Mn2 and the symmetry related Mn2' is part of two partial cubanes completed with Mn3 and the symmetry related Mn3' which are connected to Mn1 and Mn1' through the two μ-Cl bridge. One Mn(II) ion, Mn1, is pentacoordinate, while Mn2, Mn3 and Mn4 are all hexacoordinated in a distorted octahedral fashion. The JT axis of Mn2 is orthogonal to the JT axis of Mn4. The peripheral ligation is provided by bridging carboxylates and phenoxo groups from SALO ligands and terminal MeOH and H_2O groups. The SALO ligands in complex **1** display the modes of coordination I, II and III, as shown in Scheme 1, bridging two, three and four Mn ions. The protonation levels of the oxygen atoms from the various organic ligands were determined from a combination of charge balance considerations, inspection of bond lengths and bond valence sum (BVS) calculations, [19], tables 2 and 3.

Table 1. Crystallographic and data collection parameters for complexes **1**, **2**, and **3**.

	1·2C$_2$H$_3$N·5CH$_4$O ·2H$_2$O	**2·3CH$_3$CN·CH$_3$OH**	**3·CH$_3$CN·H$_2$O**
formula	$C_{81}H_{128}Cl_2Mn_8N_2O_{35}$	$C_{78}H_{113}Mn_2N_6Ni_2O_{20}$	$C_{72}H_{101}O_{20}N_4Mn_2Ni_2$
fw, g/mol	2198.27	1679.55	1567.45
crystal system	Triclinic	Triclinic	Monoclinic
space group	$P\bar{1}$	$P\bar{1}$	P21/c
a, Å	13.3688(11)	15.4594 (8)	16.3717 (11)
b, Å	13.4569(11)	21.7975 (11)	39.681 (3)
c, Å	15.1183(14)	27.0622 (15)	12.6690 (8)
α, deg	96.677(5)	72.911 (3)	90
β, deg	115.229(5)	79.157 (3)	110.255 (4)
γ, deg	95.465(5)	76.298 (3)	90
V, Å^3	2411.75	8399.4 (8)	7721.4 (9)
Z	2	1	4
D_{calc}, g/cm^3	1.378	1.325	1.352
μ, mm^{-1}	1.137	0.81	0.85
T, K	100	101	101
unique reflections	7356	48894	14750
w*R*2 (all data)	0.184	0.200	0.165
*R*1 (all data)	0.058	0.065	0.056
S (all data)	1.07	1.03	1.01

Table 2. BVSs for the Mn Atoms of cluster **1·2MeCN·5MeOH ·2H$_2$O** [a]

manganese BVSs		
atom	Mn(II)	Mn(III)
Mn1	**1.959**	1.822
Mn2	3.251	**2.974**
Mn3	**2.024**	1.893
Mn4	3.247	**2.969**

[a] The bold value is the closest one to the charge for which it was calculated.

Table xx . BVSs for selected O Atoms of cluster **1·2MeCN·5MeOH·2H$_2$O** [b]

oxygen BVSs				oxygen BVSs			
atom	BVS	assignment	group	atom	BVS	assignment	group
O1	1.976	SALOH	Ar(OH)COO**H**	O9	1.910	SALOH	Ar(OH)COO**H**
O2	1.914	SALO	Ar(O**H**)COOH	O10	1.853	SALO	Ar(O**H**)COOH
O3	2.079	O^{2-}	O^{2-}	O13	1.177	MeOH	RO**H**
O8	2.048	MeO^-	RO**H**	O14	0.434	H_2O	H_2O

[b] The BVS values for O atoms of O^{2-}, OH^-, and H_2O groups are typically 1.8 – 2.0, 1.0 – 1.2, and 0.2 – 0.4, respectively, but can be affected by hydrogen bonding.

$[Pr_2NH_2][Mn_2Ni_2(OH)_2(L_1)_2(SALO)_2(SALOH)_3]$ (**2**) crystallizes in the Triclinic space group P-1. The asymmetric unit consists of two $[Mn_2Ni_2]$ anions, the two dipropylammonium cations and solvent molecules.

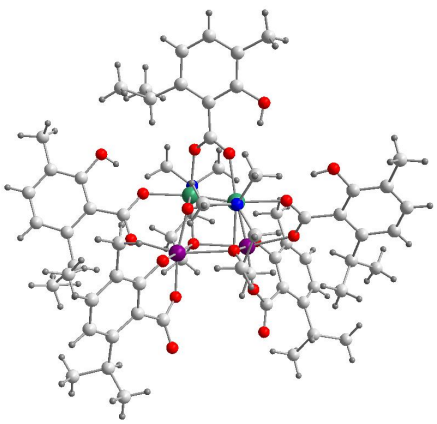

Figure 2. Crystal structure of complex **2**. Carbon: grey, hydrogen: light grey, oxygen: red, N: blue, Ni(II): green, Mn(III): purple (color online).

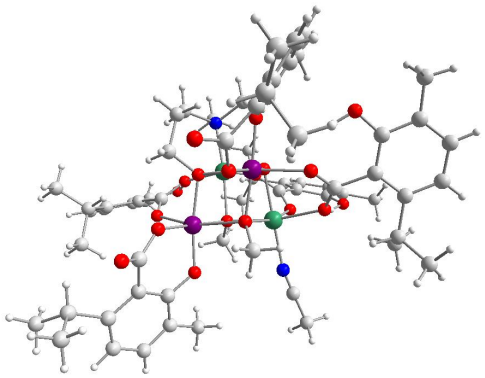

Figure 3. Crystal structure of complex **3**. Carbon: grey, hydrogen: light grey, oxygen: red, N: blue, Ni(II): green, Mn(III): purple (color online).

The two molecules in the asymmetric unit are isostructural, and only one will be described. The crystal structure of one of the two isostructural anions that compose the asymmetric unit of the crystallographic structure of complex **2**, is shown in Figure 2. The core of the $[Mn_2Ni_2]$ anion of complex **2** consists of a distorted heterometallic cubane composed of two Mn(III) and two Ni(II) ions with two μ_3-OH and two μ_3-O from the aminoalcohol ligands. The Ni-O-Ni angles are between 94.72º to 94.46º, the Mn-O-Ni angles have values between 101.22 to 99.26º and the Mn-O-Mn angles have values from 101.59º to 101.70º. The Mn and Ni sites were assigned based on the Jahn-Teller distortion observed for the Mn(III) centers and the bond distances. The oxidation states were confirmed by bond-valence sum calculations, (SI, Tables XX). All the metal centers are hexacoordinated in a distorted octahedral environment. In complex **2**, two bridging aminoalcohol ligands have been incorporated to the product. These ligands bind one Ni(II) ion with N-donor and two Mn(III) and a Ni(II) with the oxygen donor atom, which is part of the $[Mn_2Ni_2O_4]$ cubane core, the other two triply bridging oxygen atoms in the core are provided by hydroxo ligands. The four metal centers complete their coordination spheres with two SALO and three SALOH ligands in the coordination modes IV and VI, as shown in Scheme 1. Complex **3** crystallizes in the Monoclinic space group P21/c. The asymmetric unit is comprised of one $[Mn_2Ni_2O_4]$ anion, a dipropylammonium cation and crystallization solvent molecules. The crystal structure of complex **3**, $[Pr_2NH_2][Mn_2Ni_2(OH)(OMe)_2(L_1)(MeCN)(SALO)_2(SALOH)_3]$ is shown in Figure 3. The $[Mn_2Ni_2O_4]$ core of complex **3** is very similar to that of complex **2**, but in complex **3** two triply bridging oxo modes are from methoxo ligands, one is from a hydroxo ligand and the last triply bridging oxo is from a bridging aminoalcohol ligand. The main difference between complex **3** and complex **2** is the number of aminoalcohol ligands incorporated to the complex: two for complex **2** and only one for complex **3**. The Mn and Ni sites were assigned based on the Jahn-Teller distortion observed for the Mn(III) centers and the bond distances. The oxidation states were confirmed by bond-valence sum calculations, (SI, Tables XX). All the metal centers are hexacoordinated in a distorted octahedral environment. To complete the hexacoordination, Ni(2) has a terminal acetonitrile molecule. The salicylato ligands display the same coordination modes IV and VI found in complex **2**.

3.3 Magnetic properties

Magnetic susceptibility data were collected on crushed microcrystalline samples of complexes **1** and **3** in the 2.0-300 K range at applied dc fields of 0.3 T. The data for complexes **1** and **3** are shown in Figure 4 as a χT vs. T plots and in Figure 5 as magnetization vs. field plots. The χT product for complex **1** has a value of 28.24 cm^3 K mol^{-1} at 300 K, in good agreement with the spin-only value for four non-interacting Mn(III) atoms with S = 2 and four Mn(II) atoms with S = 5/2 (g = 2.0, χT = 29.50 cm^3 K mol^{-1}). As temperature decreases, the χT product gradually decreases to 4.30 cm^3 K mol^{-1} at 2.0 K, indicating antiferromagnetic coupling between the manganese ions in the complex. As temperature decreases, the Boltzman population of the excited states with large S values decreases while the low S value antiferromagnetically coupled ground state is populated. The magnetization vs. field plot for complex **1**, shown in Figure 5 clearly displays no saturation even at 5 T. This is typical of complex with a low spin ground state and accessible, low energy excited states [20]. Complex **1** has a low spin ground state and is expected to have small anisotropy due to the orthogonal arrangement of the JT axes on the Mn(III) ions, thus as expected no out-of-phase ac magnetic susceptibility signal was observed for this sample.

The χT product for **2** at 300 K has a value of 7.8 cm^3 K mol^{-1}, in good agreement with the spin–only value (for two non–interacting Mn(III) ions and two Ni(II) ions g = 2.0, χ_MT = 8.00 cm^3 K mol^{-1}). As temperature decreases, so does the χT product, indicating antiferromagnetic coupling between the metal centers, leading to a low spin ground state. This is confirmed by the lack of saturation of the magnetization vs. field measurements at 2 K, shown in Figure 5. A Van Vleck equation can be written for complex **2** using the spin Hamiltonian shown in Equation 1, where Mn1, Mn2, Ni1 and Ni2 refer to the metal sites are shown in Scheme 2. Using this equation, the experimental susceptibility data could be fitted, with the best fitting shown in Figure 4 as a solid line. The best fitting parameters were g = 2.11, J(Ni-Ni) = 0.77 cm^{-1}, J(Mn-Mn) = -5.59 cm^{-1} and J(Mn-Ni) = -2.70 cm^{-1}. These exchange coupling parameters are in agreement with the structural features of complex **2** and lead to a non-isolated spin ground state, as reflected in the magnetization vs. field plot, shown in Figure 5.

CAMBIAR ESTA FIGURA

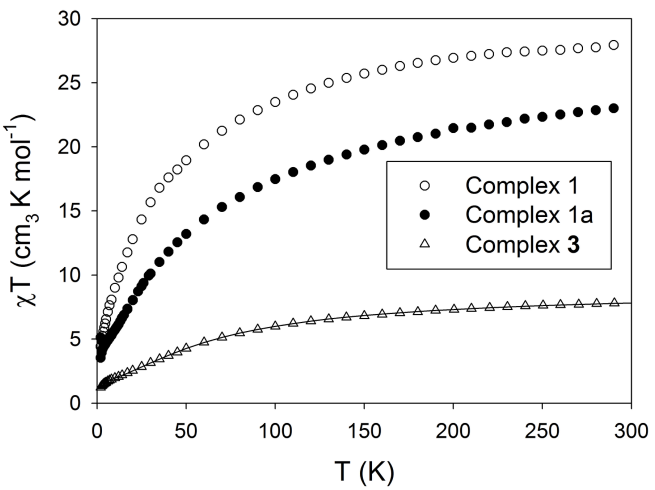

Figure 4. Magnetic susceptibility shown as χT vs. T plots for complexes **1** and **2**. The solid line is the best fit to the experimental data for complex **2** using Eq. 1. See text for fitting parameters.

Equation 1. $\mathcal{H} = -2\,J(Ni-Ni)\left[\hat{S}(Ni1)\cdot\hat{S}(Ni2)\right] - 2\,J(Mn-Mn)\left[\hat{S}(Mn1)\cdot\hat{S}(Mn2)\right] - 2\,J(Mn-Ni)\left[\hat{S}(Ni1)\cdot\hat{S}(Mn1) + \hat{S}(Ni1)\cdot\hat{S}(Mn2) + \hat{S}(Ni2)\cdot\hat{S}(Mn1) + \hat{S}(Ni2)\cdot\hat{S}(Mn2)\right]$

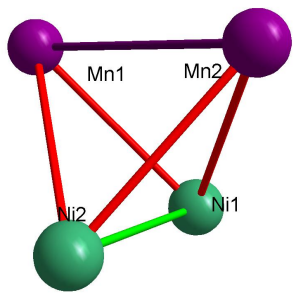

Scheme 2

CAMBIAR ESTA FIGURA

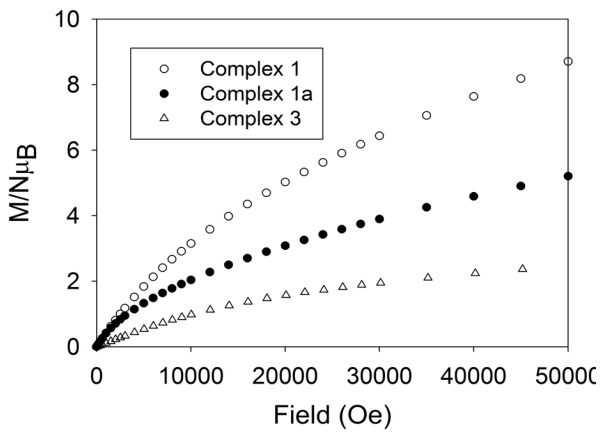

Figure 5. Magnetization vs. field plots for complexes **1**, **1a** and **3** measured at 2.0 K.

3. Conclusions

A comparative study of microwave assisted reactions vs. bench top reactions for Mn/salicylato and Mn/Ni/salicylato systems have been performed. The results reported here show that for the homometallic Mn system the microwave assisted synthesis presents the advantages of shorter reactions times and high phase purity of the obtained products while for an heterometallic Mn/Ni system the products obtained by microwave assisted synthesis are different to those obtained in bench-top conditions. Clearly, the main effect of microwave assisted heating in the Mn/salicylate system is to stop the formation of insoluble manganese oxides and to greatly improve product purity. In the case of complex **1** the bench-top reactions afforded mixtures of products with manganese oxides that were impossible to purify while the microwave reactions afforded pure products in crystalline form. However, in the heterometallic reaction systems of Mn/Ni the synthetic method used determines the product. In this example, microwave assisted synthesis has failed in facilitating the isolation of a pure product and the result is probably dominated by the great stability of complex **1**.

On the other hand, bench-top reaction results in new Mn_2Ni_2 cubane complexes **2** and **3**. We believe this work emphasizes the complexity of coordination chemistry and how useful microwave assisted synthesis can be to find new high-nuclearity complexes. The advantages of microwave assisted synthesis such as short reaction times, access to new species, great phase purity of the obtained products and very limited amount of residues make this methodology an indispensable tool for coordination chemists.

Acknowledgements

ECS acknowledges the financial support from the Spanish Government, (Grant CTQ2009-06959 and Ramón y Cajal contract). M.L.G. acknowledges the support from Oficina de Asuntos Internacionales, Centro de Electroquímica y Energía Química, CELEQ, and Escuela de Química de la Universidad de Costa Rica for financing six months research stay at the Universitat de Barcelona, and the Vicerrectoría de Investigación which partially supported this work by the project Nº 115-B1-168.

Appendix A. Supplementary Information

Cif files can be obtained free of charge from the Cambridge Crystallographic Data Centre (https://www.ccdc.cam.ac.uk/), with deposition codes 962400 (complex **3**), 962402 (complex **1**) and 962403 (complex **2**)

Electronic Supplementary Information (ESI) available: [details of any supplementary information available should be included here]. See DOI: 10.1039/b000000x/

Notes and references

[a] Departament de Química Inorgànica and Institut de Nanociència i Nanotecnologia, Universitat de Barcelona, Diagonal 645, 08028 Barcelona Spain.

[b] Centro de Electroquímica y Energía Química (CELEQ) and Escuela de Química, Universidad de Costa Rica, San José, Costa Rica.

[1] T. Lis, *Acta Cryst. B36* (1980) 2042.

[2] (a) R. Sessoli, H–L. Tsai, A. R. Schake, S. Wang, J. B. Vincent, K. Folting, D. Gatteschi, G. Christou, D. N. Hendrickson, *J. Am. Chem. Soc.* 115 (1993) 1804. (b) D. Gatteschi, A. Caneschi, L. Pardi, R. Sessoli, *Science*. 265 (1994) 1054.

[3] (a) R. Sessoli, D. Gatteschi, A. Caneschi, M. A. Novak, *Nature.* 365 (1993) 141. (b) H. J. Eppley, H. L. Tsai, N. de Vries, K. Folting, G. Christou, D. N. Hendrickson, *J. Am. Chem. Soc.* 117 (1995) 301. (c) P. C. E. Stamp, A. Gaita–Ariño, *J. Mater. Chem*. 19 (2009) 1718. (d) J. Lehmann, A. Gaita–Ariño, E. Coronado, D. Loss, *J. Mater. Chem.* 19 (2009) 1672. (e) G. A. Timco, S. Carretta, F. Troiani, F.

Tuna, R. J. Pritchard, C. A. Muryn, E. J. L. McInnes, A. Ghirri, A. Candini, P. Santini, G. Amoretti, M. Affronte, R. E. P. Winpenny, *Nat. Nanotechnol*. 4 (2009) 173. (e) E. C. Sañudo, T. Cauchy, E. Ruiz, R. H. Laye, O. Roubeau, J. T. Simon, G. Aromí, *Inorg. Chem.* 46 (2007) 9045. (f) L. Bogani, W. Wernsdorfer, *Nat. Mater*. **7** (2008) 179.

[4] R. E. P. Winpenny, *J. Chem. Soc., Dalton Trans*. (2002) 1.

[5] R. H. Laye, E. J. L. McInnes, *Eur. J. Inorg. Chem.* (2004) 2811.

[6] C. O. Kappe, B. Pieber, D. Dallinger, *Angew. Chem. Int. Ed.* 51 (2012) 2.

[7] (a) S. A. Galema, *Chem. Soc. Rev*. 26 (1997) 233. (b) C. O. Kappe, *Chem. Soc. Rev.* 37 (2008) 1127.

[8] J. Klinowski, F. A. Almeida, P. P. Silva, J. Rocha, *Dalton Trans.* 40 (2011) 321.

[9] Y. Yoo, H–K. Jeong, *Chem. Commun*. (2008) 2441.

[10] Z. Lin, D. S. Wragg, R. E. Morris, *Chem. Commun*. (2006) 2021.

[11] A. H. Jhung, T. Jin, Y. K. Hwang, J–S. Chang, *Chem. Eur. J*. 13 (2007) 4410.

[12] (a) C. J. Millos, A. Prescimone, J. Sánchez–Benítez, S. Parsons, M. Murrie, E. K. Brechin, *Inorg. Chem*. 45 (2006) 7053. C. J. Millos, A. Vinolova, G. Whittaker, S. Parson, W. Wernsdorfer, G. Christou, S. P. Perlepes, E. K. Brechin, *Inorg. Chem*. 45 (2006) 5272. I. A.; Gass, C. J. Millos, G. Whittaker, F. P. A. Fabiani, S. Parson, M. Murrie, S. P. Perlepes, E. K. Brechin, *Inorg. Chem*. 45 (2006) 5281.

[13] A. Pons–Balagué, N. Ioanidis, W. Wernsdorfer, A. Yamagushi, E. C. Sañudo, *Dalton Trans*. 40 (2011) 11765.

[14] A. Pons–Balagué, M. J. Heras–Ojea, M. Ledezma–Gairaud, D. Reta–Mañeru, J. S. Teat, J. Sánchez–Costa, G. Aromí, E. C. Sañudo, *Polyhedro.* 52 (2013) 781**.**

[15] M. Ledezma–Gairaud, L. W. Pineda, G. Aromí, E. C. Sañudo, *Polyhedron*. 64 (2013) 45.

[16] M. A. Halcrow, J–S. Sun, J. C. Huffman, G. Christou, *Inorg. Chem*. 34 (1995) 4167.

[17] A. Pons–Balagué, S. Piligkos, S. J. Teat, J. Sánchez–Costa, M. Shiddiq, S. Hill, G. Castro, P. Ferrer–Escorihuela, E. C. Sañudo, *Chemistry, Eur. J*. 19 (2013) 9064.

[18] A. Escuer, G. Aromí, *Eur. J. Inorg. Chem.* (2006) 4721.

[19] (a) I. D. Brown, R. D. Shannon, *Acta Cryst.* A29 (1973) 266. (b) I. D. Brown, D. Altermatt, *Acta Cryst.* B41 (1985) 244. (c) I. D. Brown, K. Kun Wu, *Acta Cryst*. B32 (1976) 1957.

[20] (a) E. C. Sañudo, V. A. Grillo, M. J. Knapp, J. C. Bollinger, J. C. Huffman, D. N. Hendrickson, G. Christou, *Inorg. Chem*. 41 (2002) 2441. (b) E. J. Seddon, J. Yoo, K. Folting, J. C. Huffman, D. N. Hendrickson, G. Christou, *J. Chem. Soc., Dalton Trans. (*2000**)** 3640. E. C. Sañudo, W. Wernsdorfer, K. A. Abboud, G. Christou, *Inorg. Chem.* 43 (2004*)* 4137.